SANSA - Hybrid Terrestrial-Satellite Backhaul Network: Scenarios, Use cases, KPIs, Architecture, Network and Physical Layer Techniques

Authors

Georgios Ziaragkas[1] [*] [†], Georgia Poziopoulou[1], José Núñez-Martínez[2] , Jorge Baranda Hortigüela[2], Isaac Moreno[3] , Christos Tsinos[4] , Sina Maleki[4], Shree Krishna Sharma[4], Maha Alodeh[4], Symeon Chatzinotas[4]

[1] Avanti Communications Group plc, London, UK
[2] Centre Tecnològic de Telecomunicacions de Catalunya (CTTC), Barcelona, Spain
[3] Thales Alenia Space España, Madrid, Spain
[4] University of Luxembourg, Luxembourg, Luxembourg

[*] Correspondence to: Georgios Ziaragkas, Avanti Communications Group plc, Cobham House, 20 Black Friars Lane, London EC4V 6EB, UK
[†] Email: georgios.ziaragkas@avantiplc.com

Abstract— SANSA (Shared Access terrestrial-satellite backhaul Network enabled by Smart Antennas) is a project funded by the EU under the H2020 program. The main aim of SANSA is to boost the performance of mobile wireless backhaul networks in terms of capacity, energy efficiency and resilience against link failure or congestion while easing the deployment in both rural and urban areas and assuring at the same time an efficient use of the spectrum. This paper provides an overview and the first results of the project and, more specifically, it describes the regulatory environment, the State of The Art of mobile backhauling technologies regarding Ka band, the scenarios, the use cases, and the KPIs along with the SANSA architecture, network (NET), and physical (PHY) layer techniques used to enhance wireless backhauling capabilities.

Keywords—Backhaul network, terrestrial-satellite shared access; SANSA; self-organizing network; smart antennas.

1. Introduction

The changes in user trends and the appearance of new applications in recent years resulted in a huge increase of mobile traffic worldwide. Different access network technologies such as millimetre wave access, Heterogeneous networks (HetNets) or Massive MIMO have been proposed and are being currently investigated for dealing with such traffic increments. In fact, out of the targeted 1000x increase in capacity offered in the access by future 5G communication systems, one third is expected to come from increased spectral efficiency, one third from the use of additional spectrum, and the other one third is expected to come from reduced cell sizes [1].

SANSA (Shared Access terrestrial-satellite backhaul Network enabled by Smart Antennas) is a project funded by the EU under the H2020 program and is focused on providing a solution for the backhaul of future communication systems to serve such increasing traffic volumes.

The objectives of SANSA are:

- To increase the mobile backhaul networks capacity in view of the predicted traffic demands;
- To drastically improve backhaul network resilience against link failures and congestion;
- To facilitate the deployment of mobile networks both in low and highly populated areas;
- To improve the spectrum efficiency in the extended Ka band for backhaul operations;
- To reduce the energy consumption of mobile backhaul networks;
- To strengthen European terrestrial and satellite operators market and their related industries;

The solution envisaged in SANSA is a spectrum efficient self-reconfigurable hybrid terrestrial-satellite backhaul network based on three key principles: (i) a seamless integration of the satellite segment into terrestrial backhaul networks; (ii) a terrestrial wireless network capable of reconfiguring its topology according to traffic demands; (iii) a shared spectrum between satellite and terrestrial segments. The combination of these characteristics will result in a flexible solution capable of efficiently routing the mobile traffic in terms of capacity and energy consumption, while providing resilience against link failures or congestion and easy deployment in rural areas.

In this paper we are first presenting the regulatory environment, which is very important for defining the frequency range in which SANSA is going to operate in order to perform the interference analysis as well as define the interference mitigation techniques that are analysed later on, the scenarios, that are instances of the use cases that SANSA is trying to address and the KPIs that will provide the means to assess SANSA performance. Then, we present the system architecture and the two new components, the intelligent Backhaul Node and the Hybrid Network Manager (HNM), The HNM acts as the orchestrator of the system and manages the network centrally whereas the iBN is the node component that manages locally the node as described in detail in section 3. The next set of performance simulation results stem from the different scenarios based on different network conditions. In a working SANSA network the topology changes would be applied by the HNM and the iBN. Lastly the interference landscape and interference mitigation techniques are presented. Moreover a benchmark interference topology is presented. The connection to the previous presented work is that based on this analysis we can create a radio environment map and we can communicate changes to HNM in order to apply new topologies if needed. Furthermore we can use nulls in order to provide the weights for our antennas to operate with minimum interference.

The paper is structured as follows: the next section focuses on the considered scenarios, use cases and KPIs. Afterwards, the details regarding the SANSA system architecture and the NET layer techniques used are presented in Section III and Section IV respectively. The PHY layer techniques are included in Section VI. Finally, Section VII concludes the paper.

2. SANSA scenarios, use cases, KPIs

2.1 Regulatory environment

One of the important aspects for SANSA is to identify the potential bandwidth segments within the Ka band that the hybrid backhauling network can operate in. Therefore, an in depth analysis of the regulatory environment regarding the Ka band (17.7 – 20.2 GHz for the downlink and 27.5 – 30 GHz for the uplink) has been performed taking into consideration ITU, CEPT and national level regulations.

Uncoordinated satellite terminals according to the current regulatory environment in Europe can be deployed in 17.3 -20.2 GHz [2][4][5] for the downlink and in bands 27.5 - 27.8285 GHz, 28.445 – 28.9485 GHz and 29.4525 – 30 GHz [1][4][5] for the uplink . It should be noted that these bands, which are illustrated in Figure 1, represent the maximum available bandwidth for uncoordinated satellite terminals and the actual availability will vary among different European countries depending on whether they have implemented the relevant CEPT decisions or not.

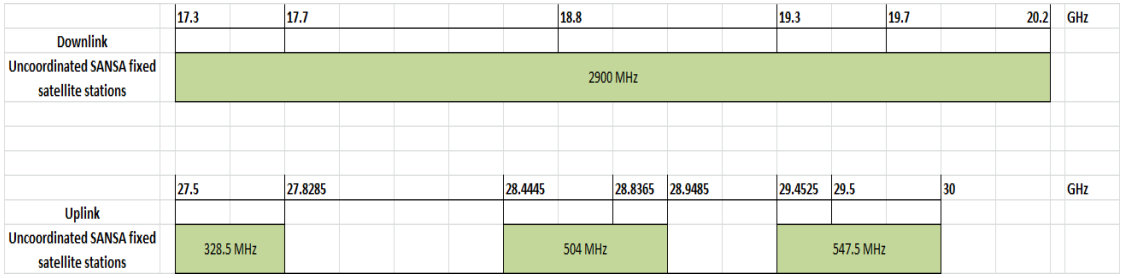

Figure 1: Maximum available bandwidth for uncoordinated FSS stations based on CEPT implementations

Apart from the frequency band that SANSA can operate in, it is important to investigate the licensing procedure for the SANSA backhaul links. In the regulatory analysis that was carried out at the beginning of the project five types were identified: individual licensing per link, block spectrum assignment, lightly licensed spectrum, shared license and unlicensed spectrum. The analysis showed that about 65.5% of backhaul links have been registered on a per link license, especially the point-to-point (P2P) links in 18 GHz to 42 GHz. However, the use of block spectrum assignment has recently increased amounting for 20.7% of the operating links especially for point-to-multipoint (P2MP) links [39].

In 2013 the majority of operational backhaul links were traditional microwave Line of Sight (LoS) links. However, the terrestrial links are expected to extend into the millimetre bands focusing in urban deployments where the distance between links is shorter. It is estimated that backhaul links using millimetre wave technology will constitute 24% of backhaul links in 2019 [39]. The number of micro-cell deployments using both P2P and P2MP links is expected to increase especially in urban settings.

The most important findings from the regulatory and SOTA analysis [38] can be summarized as follows:

- The terrestrial antenna height ranges from 20 to 60 meters.
- The terrestrial antenna EIRP ranges from 20 to 50 dBW for P2P links in 18 GHz band.

- Channels are normally 7 MHz, 14 MHz, 28 MHz or 56 MHz. The most common are the 28 MHz channels; however in the UK there is a considerable amount of links with 7 MHz channels.
- Each P2P link has normally 1 or 2 carriers.
- Distance of P2P links on the 18 GHz band is in the order of 20 Km.
- The majority of antennas for P2P links have 3-4 degrees of beamwidth.
- The terrestrial antenna gains are usually around 32-39 dBi.
- The satellite air interface used for the FWD link is DVB-S2 whereas for the RTN link it is almost always proprietary.
- The satellite antenna dish sizes are ranging from 74cm – 2.4m depending on link budget and requirements.
- The satellite backhaul link performance with SOTA technology is 128kbps – 360Mbps in the FWD link and 128kbps – 14Mbps in the RTN link using TDM/TDMA, while with the use of SCPC in the RTN link higher data rates can be achieved.

2.2 Use cases and scenarios

Based on the project objectives that have been presented in the introduction, the following use cases have been identified for SANSA [41]:

- **Radio link failure**: In case a backhaul link fails, the network topology will be reconfigured to provide an alternative route using available satellite or terrestrial links.
- **Radio link congestion:** When backhaul links are heavily congested, SANSA network utilises the available resources to provide off-loading capabilities to the node(s) of the congested links.
- **New node deployment:** With the integration of satellite links into the backhaul network the deployment of new low cost nodes into the SANSA network becomes simple and quick.
- **Content Delivery Networks (CDN) integration:** The proposed SANSA network supports CDN caching capabilities using just satellite broadcasting or by combining satellite and terrestrial caching of edge nodes.
- **Remote cell connectivity:** The hybrid SANSA network can connect isolated sites such as very rural areas or moving vessels to the mobile backhaul network with the use of the satellite links.

The periodicity of these events is an important characteristic of the use cases presented above has a significant impact on the network design. We have identified three types of events based on their frequency; periodic, semi-periodic and rarely occurring events. As periodic, we classify a regular event such as the high traffic demand during working hours in specific areas. An event that occurs on an almost periodic basis (e.g. a football match) is referred to as a semi-periodic event and lastly a unique event that will not be repeated (e.g. a concert) is a rarely occurring event. Apart from these types of periodicity, there is also the seasonality of the traffic demands. For instance, summer and winter resorts are subject to significant seasonal changes in traffic demands.

Based on the use cases identified we moved on to define appropriate SANSA scenarios. These scenarios will be used to study the mechanisms developed by the project. A 5-axes methodology was followed to fully define the scenarios which are summarised in Table 1.

The first step is to define the segment of the Ka band shared spectrum that will be utilised. According to Figure 1, spectrum sharing occurs at the downlink (DL), the uplink (UL) or both the DL and UL. The main focus in the selected scenarios is the sharing only in the DL for two reasons; the first being current regulations do not allow sharing in the UL, and the second that there is a greater need to increase the available bandwidth in the DL due to the increasing asymmetry between the two directions (FWD:RTN ratio). Two scenarios where both UL and DL spectrum sharing exists are included to enrich the research on the interference mitigation techniques explored for the SANSA network.

The next step is the definition of the carrier bandwidth for the satellite backhaul links. The SOTA carrier sizes (DL 54 MHz and UL 9 MHz) will be used for the majority of the scenarios, however another two schemes are considered to ensure alignment with the 2020 timeframe. The other two options regarding the carrier bandwidth are based on the BATS project [37](DL 421 MHz and UL 21.7 MHz) and the Ultra-Wide band (UWB) transponder(DL 230 MHz and UL 9 MHz).

The type of deployment is another scenario characteristic that needs to be specified. There are three possible types of deployment; urban, rural and mobile platform. Urban scenarios are characterised by high node density, high traffic demand and good access to high speed optical fibre networks. In contrast, rural scenarios refer to areas with low population density served mainly by microwave links and without access to fixed high speed backhaul infrastructure. The third type of deployment is the mobile platform such as cruise ships that need satellite connectivity while cruising out in the sea but could have access to terrestrial infrastructure while at bay.

Another scenario characteristic is the incorporation of CDNs. As video traffic is increasing and becoming the dominant type of traffic, CDNs will become a necessity. Therefore we have selected some of the SANSA scenarios to include CDNs using two different options for cache feeding. These options are satellite multicast or satellite combined with terrestrial multicast. In these scenarios, the node design to facilitate the installation of such caching systems should be taken into account. The CDN edge caching is expected to offload significantly terrestrial networks.

Lastly, the operating frequency of the terrestrial backhaul links (18 or 28 GHz) should be selected in order for the scenarios to be considered fully defined.

2.3 End –to –end KPIs

The end-to-end key performance indicators (KPIs) that are going to be used to evaluate the SANSA network are based on the project aims and have been defined as follows:

- **Aggregated throughput:** This KPI relates directly to the project objectives and it is defined as the sum of data plane throughput that end users achieve. One of the main mechanisms used to improve the aggregated throughput will be based on a distributed intelligent routing and load balancing algorithm embedded in the intelligent backhaul nodes of the network (iBNs). It is really

important to note that aggregated throughput will result to higher user data rate at higher levels in order to translate the additional physical layer capacity into useful data rate. The focus is on selecting higher layer techniques that are not going to significantly increase overhead and throughput increase can be translated into higher data rates and increased Quality of Experience.

- **Backhaul resiliency:** This indicator refers to the ability of the hybrid SANSA backhaul network to adapt its topology in order to tackle link failures and/or congestion. This is achieved with the reconfiguration of the terrestrial links to optimise the use of available resources, and the reconfiguration of the satellite backhaul resources to provide an optimised backhaul topology.
- **Delay:** End user satisfaction is tightly related to the experienced delay when requesting a service. Although reducing delay is not one of SANSA's main goals, it is important to ensure that end user QoS requirements are fulfilled. The SANSA network will help retain an acceptable QoS regarding delay in events of link failure or congestion by employing its topology reconfiguration mechanisms and resource allocation techniques.
- **Spectrum efficiency:** This indicator is defined as the ratio of the data rate transmitted over a specific bandwidth to the bandwidth itself. The aim in the context of the project is to be able to utilise the shared Ka band for mobile backhaul. The deployment and operation of satellite and terrestrial backhaul links in the shared Ka band will be enabled with the development of novel interference mitigation techniques.
- **Energy efficiency:** Designing SANSA hybrid backhaul network with reduced power consumption compared to a conventional backhaul network is another important project aim. The traffic management algorithm with be able to exploit the knowledge of the current topology and traffic demands to allow specific nodes to go into sleep mode.
- **Coverage:** One of the SANSA objectives is to extend the mobile network deployment in rural areas that are sparsely populated and difficult to reach by taking advantage of the wide coverage that satellites offer. By showcasing the operation of this hybrid backhaul network, we will prove that the coverage of the network can be extended to 95-99% as any node within the footprint of a Ka band satellite will be able to access mobile services.

Table 2 summarises the end-to-end KPIs of the SANSA network as well as their targets.

3. SANSA Architecture

This section discusses the end-to-end system architecture of the SANSA network. The first subsection provides an overall description of the end-to-end system architecture including access, transport, and core network. This architecture aims at covering all the use cases and scenarios defined in previous section. The second subsection details the transport network architecture (TNA), which is the main focus of the SANSA project. The architecture internals of two key enabling SANSA components, the intelligent Backhaul Node (iBN) and the Hybrid Network Manager (HNM) are also presented here. Lastly, the architecture for the moving base station scenario is highlighted at the end of this section.

3.1 SANSA End-to-end System Architecture

The SANSA end-to-end system architecture encompasses the LTE-based Radio Access Network (RAN), the transport network (where the research impact resides), and the Evolved Packet Core (EPC), also referred to as core network.

The SANSA Access Architecture encompasses the mobile user equipment (UEs) and base stations (BSs), which can be either macrocells (eNodeBs/eNBs) or small cells (SCs also referred to as Home eNodeBs/HeNBs). It is important to note that both macrocells and small cells are embedded in intelligent Backhaul Nodes (iBNs) and Backhaul nodes (BNs), as can be shown in Figure 2. Since SANSA especially focuses on the transport network, all the 3GPP signalling procedures in the EPC and the RAN are adopted without modifications. A detailed description explanation of the main 3GPP building blocks and interfaces can be found in [6].

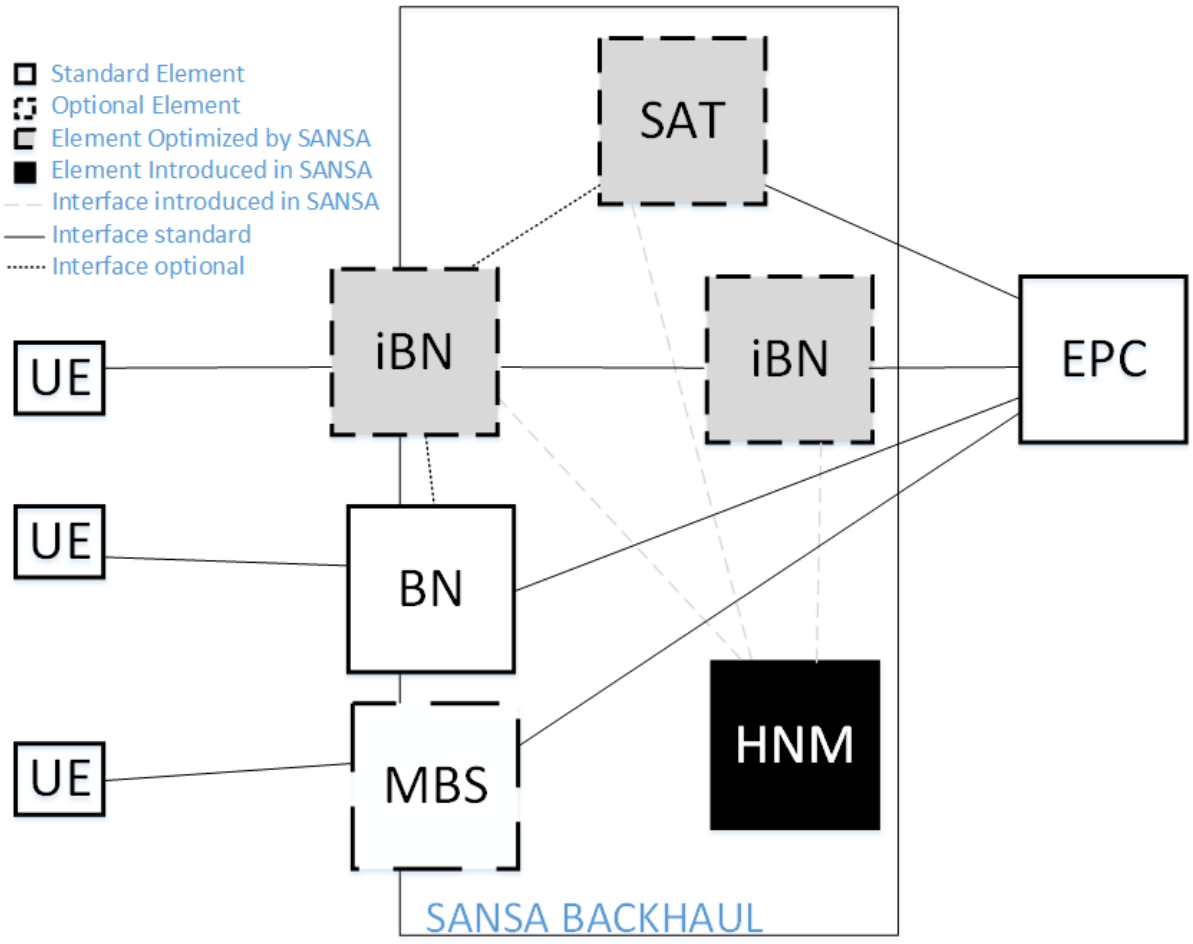

Figure 2: The SANSA end-to-end System Architecture

These entities exchange control plane procedures with the (H)eNBs by means of the S1-MME interface. In particular, the S1-AP (Application Protocol) [7] provides the necessary control message signalling between the (H)eNBs and the EPC with bearer establishment and mobility management being some of the network functions it performs. Regarding user plane traffic, they are tunnelled through various functional entities in the EPC by means of GPRS Tunnelling Protocol User Plane tunnels (GTP-U) [8] . The S1-U interface provides user plane tunnelling between the (H)eNodeBs and the EPC. The GTP-U protocol tunnels user data between

(H)eNodeBs and the EPC, and between the element inside the EPC. The goal of the GTP-U protocol is to encapsulate IP traffic in flow specific tunnels to provide QoS differentiation. The S5 interface provides user plane tunnelling between the endpoints in the EPC.

It is in the Transport Network where SANSA introduces its main research novelties. In what follows, we describe the main entities optimized and introduced by the SANSA network.

3.1.1 SANSA Backhaul Network Architecture

The SANSA system focuses on evolving the backhaul network architecture. The backhaul network is in charge of transporting data between the UEs and the EPC. The SANSA TNA combines both satellite and terrestrial transport architectures. In this sense, the SANSA transport network architecture is composed by the following key elements.

The iBN extends the internal architecture of traditional BNs by introducing new functional blocks and interfaces for the proper management of backhaul satellite and terrestrial resources. Amongst other functions, the iBN will embed routing, traffic classification, and energy management functions. The iBN will operate on short to medium timescales and is reconfigurable by the HNM. It will encompass interfaces to other iBNs, and to the EPC either directly (with a radio link) or through other iBNs. Finally, any iBN may include a direct connection to the EPC through the satellite network. Note that the mobile network layer information (e.g. traffic flow from a UE) traverses the iBNs encrypted. We assume that the iBN is a trusted component by the UEs and EPC, which has enough processing capabilities, can decrypt mobile network layer information (e.g. traffic class information) tunnelled through the S1 interfaces to conduct certain functions such as traffic classification and routing of traffic flows.

The Backhaul Node (BN) is a legacy entity embedding the H(eNB) in charge of carrying transport traffic to the EPC. It neither presents intelligent routing, traffic classification, and energy management functions. A special case of BN is that of the Mobile Base Station (MBS). The MBS is a BN that includes mobility capabilities (e.g. a BS in a train). It is an optional element in the SANSA scenarios.

The Satellite (SAT) is a component enhanced by SANSA due to its smooth integration in the reconfigurable terrestrial transport network. The SAT will encompass an interface to the EPC, and an interface to iBNs. The interface between the iBN and the SAT allows the system to access the satellite link status and use the data for traffic classification, routing, topology reconfiguration, and interference management between the satellite and terrestrial links. Information such as satellite carrier frequency, channel bandwidth, available data rate and link availability is constantly monitored by the HNM.

The HNM is a new entity introduced by SANSA which includes functionalities to manage not only satellite but also terrestrial backhaul resources. Based on global network information view based on its monitoring capabilities, the HNM is in charge of configuring the topology formed between the iBN nodes and their connection and configuration of the satellite resources. In this context, it can configure backhaul resources embedded in terrestrial iBNs, MBSs, and satellite resources. It operates on long and medium timescales.

3.1.2 Intelligent Backhaul Node (iBN) Architecture

The iBN is the component that implements the SANSA ground (or terrestrial) transport network. The iBNs, which are distributed throughout the SANSA meshed network, distribute and forward the user traffic, and perform network decisions on a short (e.g. routing) and medium (e.g. energy efficiency) time-scale basis. The iBN includes the satellite and terrestrial terminals, however the architecture contemplates the possibility of having purely terrestrial or satellite connected nodes. Every iBN includes an eNB component, but the novelty introduced within SANSA architecture consists in that some of the connections between the different nodes are dynamic. Note that this architecture does not try to replace the existing terrestrial backhauling infrastructure, but can be integrated with current deployments, i.e., including nodes consisting only in eNB elements, using static links. As illustrated by Figure 3, the iBNs integrate the following main software function: (H)eNB: This generally refers to the LTE stack corresponding to a base station, or a low-power base station (e.g. small cell). It is connected to the EPC through a backhaul network, which can be wired or wireless.

- Routing: This function includes the routing algorithm and is in charge of distributing the traffic among the different terrestrial and satellite modem interfaces.
- Traffic Classification: The Traffic Classification function is in charge of determining the mapping of traffic flows to the hybrid backhaul resources used to transport them.
- Energy Efficiency: This function is in charge of controlling access and backhaul energy consumption, therefore reducing operator's OPEX while satisfying traffic demands.

In terms of hardware equipment (also shown in Figure 3), we can highlight the following components:

- Modems: An iBN includes several terrestrial and/or a satellite modem.
- Antennas: According to the type of modem terrestrial smart antennas and/or a satellite antenna provides the air interface of the iBN.
- Beamforming network: This element mixes the outputs of the modems before passing it to the smart antenna.

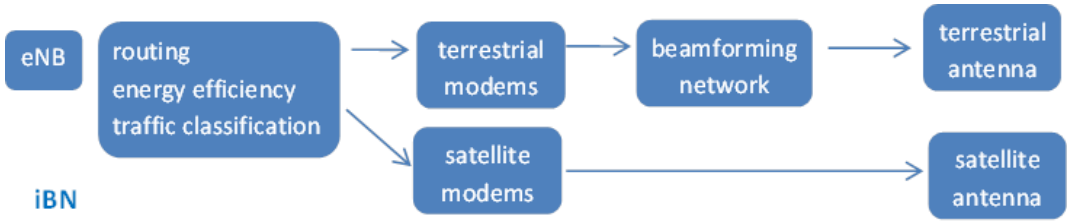

Figure 3: Intelligent Backhaul Node Architecture

3.1.3 Hybrid Network Manager (HNM) Architecture

The HNM is the central element of the SANSA network. The HNM is connected to both the iBNs and the satellite ground segment. This manager aggregates all the satellite and terrestrial backhaul resources and performs long and medium time-scale nework reconfiguration changes. In a sense, the HNM can be considered as

the SDN [40] controller implementing the control plane required to properly manage the hybrid network. According to Figure 4, it includes the following main functions:

- **Configuration management**: This function is in charge of reconfiguring the iBNs in the network to form the topology between iBNs. Configurable iBN items are for instance the terrestrial modems and antennas.
- **Events management**: This component monitors the network nodes and determines the state of SANSA network. This element is used as input for the topology management module, which is detailed below.
- **Topology management**: This module performs topology calculations to restore the hybrid network upon node congestion or failure events. As input, it receives new network states from the event management component, and produces new topologies, forwarding them to the configuration management function.

The HNM external components are:

- **Radio Environment Map**: This component calculates interference levels and performs the carrier allocation. It generates the data that can be later used by the topology management to calculate effective network throughput.
- **Satellite Ground Segment**: This component is composed by different tools for managing the satellite network, such as the Network Management System (NMS), the satellite Hub, the Operational Support Systems (OSS), and the Business Support System (BSS) for Service Provider (SP) customers.

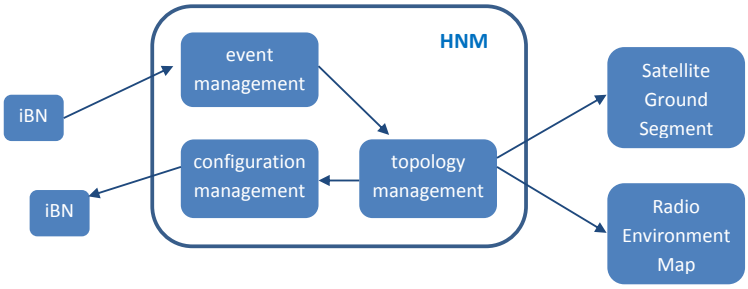

Figure 4: Hybrid Network Manager (HNM) Architecture

3.1.4 Moving Base Station Architecture

As Moving Base Station (MBS) we refer to radio access and SANSA-complied mobile backhauling infrastructure installed on a moving platform, such as a cruise ship. By SANSA-complied mobile backhauling infrastructure we mean an iBN which enables both satellite and terrestrial mobile backhauling.

Such a setup demonstrating a sailing cruise with only satellite connectivity is shown in Figure 5. The iBN could be connected terrestrially to the EPC if the cruise ship was close to terrestrial infrastructure.

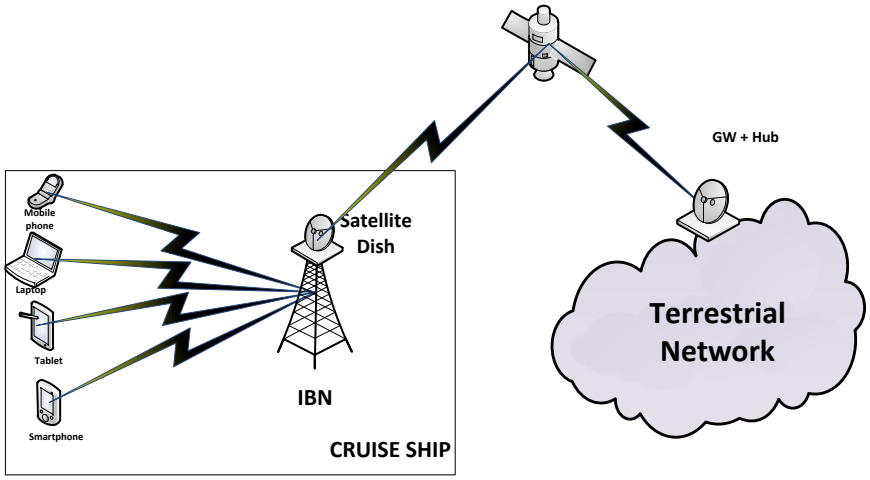

Figure 5: Moving base station architecture

4. Network layer techniques

The HNM must not only react to instant network conditions, but also solve the derived satellite-terrestrial interoperability issues. First subsection describes satellite-terrestrial interoperability issues.

Moreover, since the resulting hybrid network topology can be really complex, a dynamic routing algorithm is demanded at the node level. A self-organizing, load-balancing routing algorithm is proposed to this aim. Second subsection describes the intelligent routing functionalities embedded in the iBNs. Third subsection describes the simulation framework and the extensions implemented to fulfil SANSA simulation requirements. Finally, we provide initial results on the performance of the current simulation framework.

4.1 Network interoperability

The satellite component presence leads to several interoperability issues, when being integrated in the backhauling network, which are mainly due to the need of aggregating the available system resources. There may be some nodes having only terrestrial or satellite component, while others will be hybrid. For the last case, the satellite connectivity can be considered as a backup link, for certain network conditions, or may be used for traffic off-loading under congestion situations. Also, certain services could be preferred to be provided directly over the satellite (e.g. CDN delivery or other multicast services). The HNM must give an efficient response to any interoperability issue, diagnosing network problems new load demands, even changing/evolving network topologies (Figure 6).

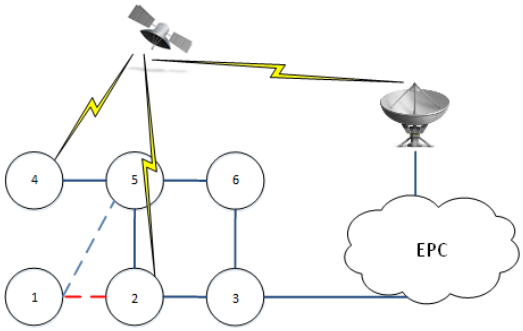

Figure 6: Interoperability

4.2 HNM Network Layer Techniques

In particular, the envisaged HMN network layer techniques are related to:

- Radio resources. This function manages the system frequency plan, interfaces with the REM tool, which will return interference levels for a certain connectivity matrix.
- Configuration management. Dedicated to remote smart antenna/modem reconfigurations. When a better topology has been calculated, the HNM can automatically perform the needed changes, or notify to the SANSA operator.
- Events management: This module performs the monitoring of the network, being in charge of detecting any state change (node interface switch on/off) or a link failure (based on modem monitored SNR values), or even a congestion situation (based on traffic level). When a network change is detected, the HNM must propose topology changes.
- Topology management. In charge of calculating, reconfiguring and distributing new network topologies to the remote nodes. Also measures the efficiency (KPI) of a certain topology. In what follows, we provide more detail on the network layer techniques followed for conducting topology reconfiguration in the HNM.

HNM Topology Reconfiguration algorithms

This algorithm will be in charge of calculation performance figures (possibly based on KPIs as throughput) for the current topology and other alternative topologies (with different connectivity matrix) that may result upon certain networking (reconfiguration) events. The HNM includes a set of ‘rules’ based on which it must perform the selection of the optimal one. The decision can be made for example, considering the best matrix as the one that gets the higher efficiency while satisfying the bandwidth requirements of the topology (or the less possible degraded behaviour). Pre-validation of candidate topologies could be assessed by external tools as the REM (in charge of calculating interference levels when using a set of carriers throughout a set of probable connectivity matrices).

Different network events must be supported as a minimum by the HNM topology algorithm rules:

- Link failure (towards a certain destination): a new link towards another neighbour node can be established. This will involve a new connectivity matrix.

- Bandwidth increase (towards the same destination): new link or carrier allocation change. Could be issued as a response to a congestion event.
- Adding a satellite link for any of the previous cases, as a response to a congestion or resiliency event.

4.3 The iBN Network layer techniques

In particular, the iBN elements are in charge of conducting the following main functions:

- Routing. An efficient a decentralized routing function, making the most out of the satellite-terrestrial wireless backhaul resources, is needed to satisfy the network scalability problem. SANSA proposes a design following the node-centric approach, in which the routes are discovered on-the-fly (i.e., on a hop-by-hop basis) while the traffic traverses the network. The backpressure algorithm described in [40] complies with these requirements and is therefore adaptable to the dynamicity of satellite-terrestrial wireless backhaul deployments.
- Traffic classification. This function is in charge of determining the mapping of traffic flows to backhaul resources used to transport them. Based on flow QoS requirements, traffic classification algorithms will determine whether to use satellite or terrestrial resource for each flow in transit.
- Energy management. The goal of the Energy Efficiency function is to control access and backhaul energy consumption, therefore reducing operator's OPEX while satisfying traffic demands. SANSA considers to tackle energy efficiency by proposing ON/OFF techniques related to both access and backhaul interfaces embedded in iBNs. In particular, when switching OFF access and terrestrial backhaul interfaces three different scenarios are contemplated:
  a) iBN is totally switched OFF (i.e., access and backhaul interface are switched OFF).
  b) iBN is switched ON with its associated access interface switched OFF. Backhaul interfaces can be used to route traffic coming from others iBNs.
  c) iBN is switched ON and all terrestrial backhaul interfaces are switched OFF. In this case, traffic will be transported through the satellite backhaul link.

4.4 The Simulation Framework

The simulation framework uses Ns-3 [35], a modular discrete-event network simulator that models SANSA network elements and includes LENA/EPC traffic simulator. It is important to highlight that in SANSA we implemented LENA extensions to allow any kind of transport topology in the data plane that connects the eNBs embedded in the iBNs and the S-GW located in the EPC. Initially, LENA did not support a backhaul infrastructure more complex than a single wired cable between each defined HeNB and the core network. In particular, we extended the LENA network simulator [36] in order to connect the previous described elements to form the hybrid backhaul network. This simulator models both the access and the core network of an LTE network. The proposed extension consists of a flexible API in the form of a new class called *HybridMeshEPCHelper* (see Figure 7), extending the *EPCHelper* class to enable the interconnection of the access and the core network segment through a more complex and custom backhaul network. The most important

method defined in this new class is *AddHybridMeshBackhaul*, which is dedicated to build and configure the hybrid backhaul network (network topology and characteristics of the terrestrial and satellite backhaul links) according to the criteria of the HNM, which is also developed within the SANSA project. Figure 7 illustrates the sequence diagram of the configuration of the hybrid mobile network.

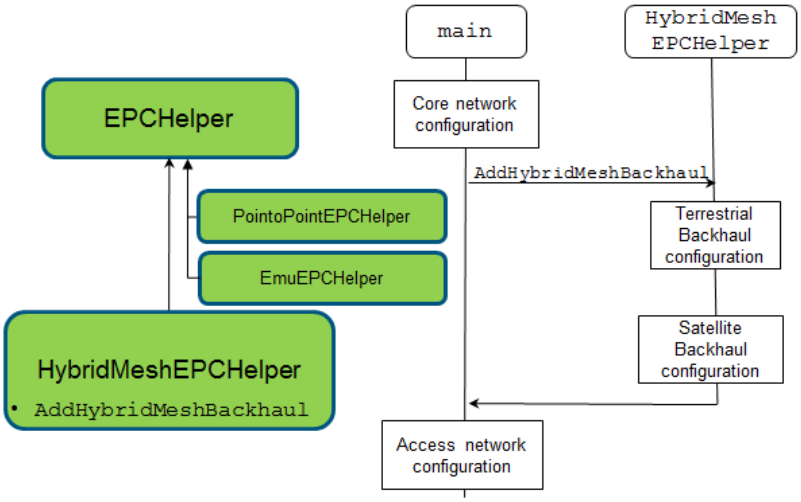

Figure 7: Implementation of LENA extensions. Sequence diagram of SANSA network configuration

The proposed extension consists of a flexible API in the form of a new class called *HybridMeshEPCHelper*, extending the *EPCHelper* class to enable the interconnection of the access and the core network segment through a more complex and custom backhaul network.

4.5 Evaluation of the Simulation Framework

Here we test and conduct an initial validation of the framework presented in previous section. The initial network deployment consists of a 2x3 grid network of iBNs with a single satellite node. Currently, the framework uses an ideal shortest path (in number of hops) routing protocol to forward traffic through the hybrid backhaul network.

LENA simulator provides an accurate model of the LTE/EPC protocol stack so the framework can be tested with ns-3 applications installed in the defined UEs which generate real LTE traffic. Note that prior to the exchange of data plane traffic, the HeNB embedded in the iBN requires to trigger 3GPP signalling procedures. User plane LTE traffic generated by UEs is tunnelled over the hybrid satellite-terrestrial mesh backhaul by means of GPRS Tunnelling Protocol User Plane tunnels (GTP-U). This protocol tunnels data between the eNodeB and the S-GW located at the EPC node. Note that, these tunnels can provide a mechanism to enforce certain policies (offloading, load balancing) for different kind of traffic flows. The work conducted in this evaluation is the first one providing LTE traffic splitted through terrestrial and satellite backhaul.

a) Satellite Offloading: Flow in the Middle

In this simulation, we illustrate the performance of a TCP flow when changing its path to arrive to the EPC. Let's imagine that the Flow1 generated by an UE arrives to the EPC using the terrestrial resources. At instant t, a new flow from this UE (Flow2) enters in the network and the iBN, at which the UE is attached, decides to change the path of Flow1 from the terrestrial to the satellite backhaul, while Flow2 reaches

the EPC using the terrestrial backhaul. Flow1 will use the terrestrial backhaul to arrive to an iBN equipped with a ST. Figure 8 shows the evolution of the throughput experienced by these flows when using Reno TCP standard-like variant. We can notice how the satellite backhaul degrades the performance of Flow1 when routed over the satellite resource, while Flow2, routed over the terrestrial network, can achieve the injected throughput. The sudden increase in round trip time (RTT) of Flow1 (around 500ms) causes retransmission time outs (RTO), which lead to an abrupt decrease of the attained throughput.

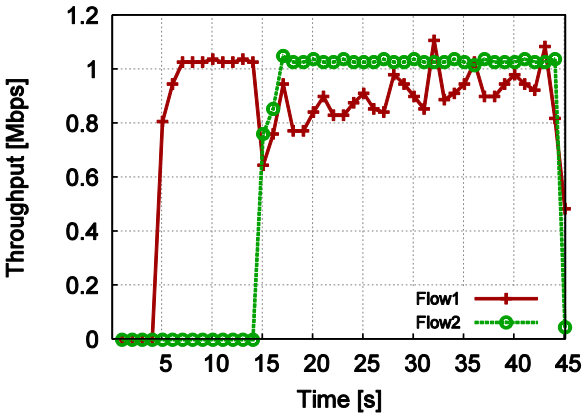

Figure 8: Satellite offloading. Achieved Throughput at the destination

An important observation is that the connectivity of Flow1 is not lost while switching to the satellite backhaul. In fact, Flow1 reaches 90% of its injected throughput after 25 seconds. In this sense, we can conclude that TCP flows without strict requirements of throughput and delay can be seamlessly transported through the satellite backhaul. Additionally, improved TCP flavours taking into account the satellite communication characteristics, like TCP Hybla [34], could improve the performance for the offloaded flows. On the other hand, this behaviour could bring significant benefits to TCP traffic flows with more strict requirements on throughput and specially on latency, because they find less congested terrestrial backhaul resources.

b) Satellite Offloading: Increasing the number of terrestrial and satellite gateways (GWs)

In this simulation, several UEs generating the same amount of traffic are attached to each iBN in the network under evaluation. Half of the traffic arriving to the iBN is mapped to reach the EPC using the satellite backhaul and the other half of the traffic reaches the EPC using only the terrestrial resources. The aim of this experiment is to see the impact on the network performance when adding progressively new STs (from zero to five) and when changing the number of iBN nodes connected to the EPC (from one to two). Notice that in this experiment, an iBN counting with connection to the EPC cannot be equipped with a Satellite. Traffic is generated to achieve network saturation conditions. The general trend is that the attained throughput will grow with the number of satellite links, but this is not always true as depicted in Figure 9. In such figure, we can observe that throughput gains are marginal when a third satellite link is added in the case of a single terrestrial GW to the EPC.

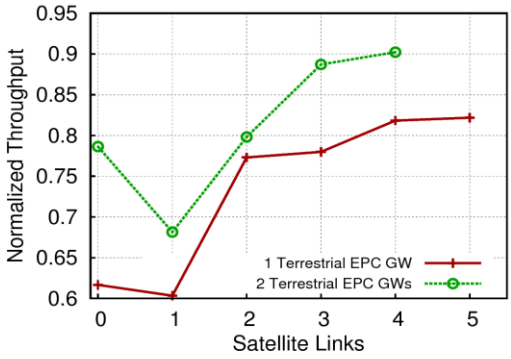

Figure 9: Normalized throughput evolution with the variation of satellite-terrestrial links connected to the EPC.

This misuse of satellite resources is due to 1) the static traffic management policy and 2) the deployment of satellite link in a non-congested zone. Furthermore, Figure 9 reveals that more resources could even translate into performance degradation. This is the case of introducing a single Satellite in the network. Both the satellite backhaul network and the allocation of terrestrial resources to reach the satellite backhaul get congested due to this static traffic management policy.

Two conclusions can be extracted from this simulation. First, additional resources may be carefully planned for an efficient exploitation so its deployment brings significant improvements to compensate the additional CAPEX expenditures. Second, rather than static traffic allocation techniques, dynamic traffic management and load balancing strategies are required to exploit these additional deployed resources.

5. PHY layer techniques

5.1 SANSA Interference Landscape

In this subsection, we consider all the possible sources of interference at the backhaul node level and access where they are relevant to the SANSA network. It is important to note that in the context of the project we refer to co-channel interference i.e. the interference caused by two or more transmitters using the same frequency.

Considering the SANSA network as a system, we distinguish interference in intra- and inter-system interference. Intra-system interference is caused by transmitters that belong to the SANSA system, whereas Inter-system interference can be caused by terrestrial and/or satellite links operating at the same frequencies from different operators than SANSA operator. The possible sources of interference are illustrated in Figure 10. Below, we explain outline the underlying intra-system interference in detail.

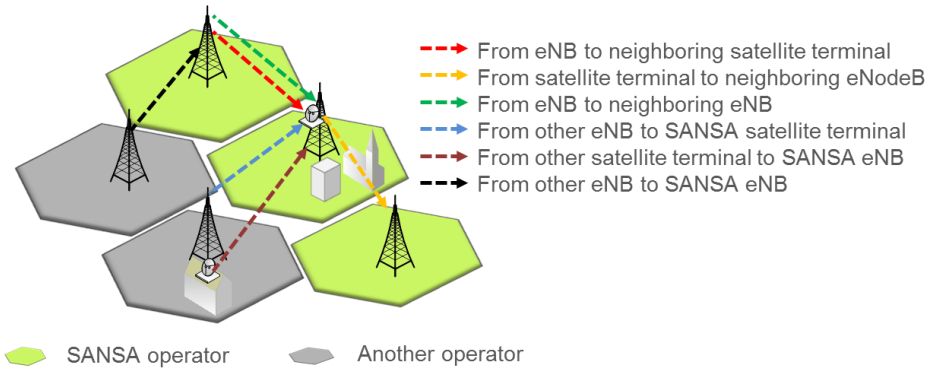

Figure 10: Interference landscape in the SANSA system

5.1.1 Intra-system interference

The intra-system interference can be either between the satellite and terrestrial links or only between the terrestrial links.

Interference between satellite and terrestrial links

Based on the spectrum sharing schemes between the satellite and terrestrial links that have been identified for the different scenarios in Figure 10, the possible causes of interference are (DL denotes downlink and UL denotes uplink):

- From eNodeB (eNB) to neighbouring satellite terminal (DL): This is the main case of interference relevant to all the defined scenarios where spectrum sharing is implemented between the satellite DL and the terrestrial links.
- From eNB to neighboring satellite terminal (UL): This case of interference is valid if there is shared spectrum between the satellite uplink and the terrestrial links which is not possible under the current regulatory environment.
- From satellite terminal to neighbouring eNodeB (UL): This case of interference is valid if there is shared spectrum between the satellite uplink and the terrestrial links which is not possible under the current regulatory environment. There are only two long term scenarios (Rural 2 and Urban 3) that are using this case of spectrum sharing and are scenarios that are not supported by the current regulatory environment but will the coexistence and deployment of terrestrial and satellite links in Ka band and specifically in 27.8285 GHz – 28.4445 GHz and 28.9485 GHz – 29.4525 GHz.
- From satellite terminal to neighbouring eNB (DL): In this case there is no interference from the satellite terminal to the eNB as the satellite terminal is only receiving at the shared frequency and not transmitting.

Terrestrial to terrestrial link

Apart from the interference mitigation techniques that enable spectrum sharing between the satellite and terrestrial links, it is important to investigate solutions for interference between terrestrial links in the SANSA network. The main technique used for this will be appropriate frequency reuse schemes depending on available spectrum resources.

5.2 Interference Mitigation and Management Techniques and Research Challenges

5.2.1 Symbol-Level Precoding

The main idea of symbol-level precoding (SLP) in the downlink is based on exploiting the interference in single node to multi-node multiple antenna system. SLP aims at

jointly utilize the spatial cross-coupling between the multi-nodes' channel and the received symbols which depend on both channel state and transmitted symbols. When untreated, this cross-coupling leads to interference among the symbol streams of the nodes. Several spatial processing techniques decouple the multi-node transmissions to reduce the interference power received at each terminal [9][10]. On the other hand, [11][12] classify the interference in the scenario of BPSK and QPSK into two types: constructive and destructive. Based on this classification, a selective channel inversion scheme is proposed to cancel the destructive interference while retaining the constructive one to be received at the nodes' terminal. A more elaborated scheme is proposed in [11][12], which rotate the destructive interference to be received as useful signal with the constructive one. These schemes outperform the conventional precoding schemes [9] and show considerable gains. However, the anticipated gains come at the expense of additional complexity at the system design level. In symbol level precoding the precoder should be updated every symbol period. Therefore, faster precoder calculation and switching is needed in the symbol-level precoding which can be translated to more complex and expensive hardware. In this direction, [13][14] proposed a symbol based precoding to exploit the interference by establishing the connection between the constructive interference precoding and multicast. Moreover, several constructive interference precoding schemes have been proposed in [13], including Maximum ratio transmission (MRT)-based algorithm and objective driven constructive interference techniques. Many metrics are addressed such as minimizing transmit power under SINR constraint, maximizing the minimum SNR and maximizing the sum rate.

The works [13][20] have shown that in symbol-level precoding more efficient solutions can be found while designing the transmitted signal directly. Following this intuition, a novel multicast-based symbol-level precoding technique was initially proposed in [13] and later elaborated in for MPSK modulations. In more detail, the transmitted signal can be designed directly by solving an equivalent PHY multicasting problem with additional phase constraints on the received user signal. Subsequently, the calculated complex coefficients can be utilized to modulate directly the output of each antenna instead of multiplying the desired node symbol vector with a precoding matrix.

Going one step further, the above techniques were generalized in [15][16] taking into account that the desired MPSK symbol does not have to be constrained by a strict phase constraint for the received signal, as long as it remains in the correct detection region. The flexible phase constraints can obviously introduce a higher SER if not properly designed. In this direction the work in [16] studies the optimal operating point in terms of flexible phase constraints that maximizes the system energy efficiency.

The previous contributions [11]-[17] focus on single-amplitude modulations, the extension to multi-level modulation is proposed in [18]-[20], where a generalized relation between the SLP for any modulations and the physical-layer multicasting is established. Moreover, a transmitter architecture that accommodates the SLP precoding techniques is proposed in [20]. Generally, the gains in SLP Precoding have similar trends to PHY-layer multicasting for any modulation [21], the required power to satisfy per user quality of service targets decreases with the system size. This means that the performance of the system enhances with more interference. This result contradicts the conventional the multi-node precoding, in which the

interference saturates the performance, therefore, the required power increases with system size [10]. Exploiting the symbol-level definition, we can formulate the optimization problem

$$w_k = \arg\min \left\| \sum_{k=1}^{K} w_k d_k \right\|^2$$
$$s.t \frac{\left| h_k \sum_{i=1}^{K} w_i d_i \right|^2}{\sigma^2} \geq \zeta_k$$
$$\angle h_k \sum_{i=1}^{K} w_i d_i = \angle d_k$$

where h_k is the channel between the transmitter and the k^{th} user, w_k is the precoding designed at the transmitter that carries the symbol d_k to serve user k, ζ_k is SNR threshold that should be satisfied and $\angle$ denotes the angle . The previous optimization can be reformulated as:

$$x = \arg\min \|x\|^2$$
$$s.t \frac{|h_k x|^2}{\sigma^2} \geq \zeta_k$$
$$\angle h_k x = \angle d_k$$

Finally, the symbol-level precoding designs the output vector x that modulates the output of each antenna, rather than designing an individual precoder for each user. This simplifies the architecture of the transmitter from the hardware perspective but complicates it from the software perspective to handle the symbol-level processing of the system. Therefore, employing symbol-level precoding does not require to change the air interface of the transmitters in the current communications systems.

The optimal multiuser MISO beamforming can be defined as [10]

$$w_1, ..., w_K = \arg\min \sum_{k=1}^{K} \|w_k\|^2$$
$$s.t \frac{|h_k w_k|^2}{\sum_{i \neq k} |h_k w_i|^2 + \sigma^2} \geq \zeta_k, \forall k \in K$$

Assuming perfect channel state information acquisition, Figure 11 compares the performance between optimal user-level beamforming, and symbol-level precoding from an average transmit power perspective. In all cases, the power minimization under SINR constraints is considered. It can be noted that symbol-level precoding (CIPM) outperforms the optimal user-level precoding at every SINR target. This can be explained by the way we tackle the interference. In OB, the interference is mitigated to grant the SINR target constraints. In CIPM, the interference is exploited at each symbol to reduce the required power to achieve the SINR targets.

Furthermore, it can be noted that the throughput of CIPM can be scaled with the SINR target by employing adaptive multi-level modulation (4/8/16-QAM).

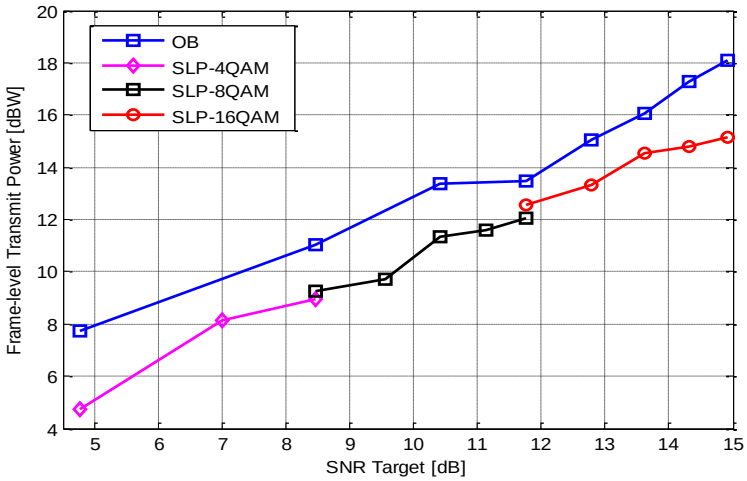

Figure 11: Frame-level Transmit Power in dBW vs target SINR in dB σ_h^2 = 10 dB, σ_z^2 = 0 dB

5.2.2 Multicasting

Multicasting refers to sending one stream of information to multiple receivers through multiple antennas. This technique is only relevant for unidirectional content delivery at the edge Base stations and is not applicable to the mobile bidirectional backhauling. Here, it is worth distinguishing two cases: 1) the same information has to be multicasted to all edge BSs (global content), 2) different streams of information have to be multicasted to each group of edge BSs (local content). For the former case, the beamforming design is based on PHY-multicasting [21], while for the latter case on PHY-multigroup multicasting [22]. It should be noted that these techniques are applicable for the terrestrial backhauling with multiple antennas at the BS or for the satellite backhauling if multibeam satellites with full frequency reuse are available. Figure 12 shows the performance of multigroup multicasting techniques for a full-frequency Ka-band satellite scenario in comparison to 4 colour frequency reuse. The maxmin fair solution achieves the same throughput towards all groups while the Sum Rate (SR) solutions maximize the system throughput. It should be noted that SRA stands for Sum-rate maximization with availability constraints, while SRM takes into account realistic DVB-S2X modcod spectral efficiencies.

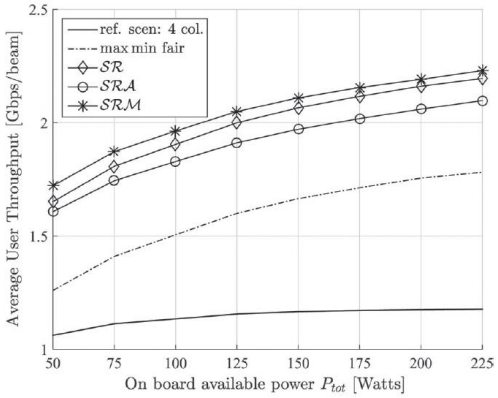

Figure 12: Performance of multigroup multicasting techniques for a full-frequency Ka-band satellite scenario in comparison to 4 colour frequency reuse.

5.2.3 3D Beamforming

Recently, three dimensional (3D) BF has been proposed as a promising candidate technique for the fifth generation (5G) of wireless systems [23]. The recent technological advancements in adaptive and flexible antenna structures/technologies have led to the possibility of designing a fully dynamic antenna pattern which can be specified as per resource block and as per user equipment, thus making 3D beamforming practically feasible [24]. In contrast to the traditional 2D beamforming, the 3D beamforming controls the radiation beam pattern in both elevation and azimuth planes, thus providing additional degrees of freedom (dofs) in the elevation plane while designing a wireless system. For this purpose, a two dimensional (2D) array structure is required in many cases in contrast to the single-dimensional (1D) array in the conventional 2D beamforming. In this direction, some lab and field trials have been carried out and the potential of 3D beamforming has been demonstrated [25]. From the presented initial results in the literature, significant improvements of the system performance have been noted with respect to the capability to separate two signals sharing the same radio resources by exploiting the advantage of reflections from building, walls and other strong reflectors.

The main benefit in terms of the average user rate comes from the fact that 3D BF can enhance the desired signal strength by pointing the vertical main lobe directly at the user terminal at any location. Besides, it reduces the strength of the inter-cell interference when serving users are closer to the base station. The beam pattern adaptation in the vertical dimension has the capability to exploit additional diversity or spatial separation, which can be subsequently used to either improve signal quality or increase the number of simultaneously served users. Authors in [26] have analyzed the standard Capon method in the 3D case with a planar array configuration, in which the Direction of Arrival (DoA) is characterized by both azimuth and elevation angles. Moreover, authors in [28] analysed the performance of the following 3D beamforming scenarios for LTE-advanced systems: (i) vertical sectorization with the same carrier frequency, (ii) vertical sectorization with different carrier frequencies based on carrier aggregation, and (iii) user-specific elevation beamforming. It has been concluded that the latter two scenarios both can achieve good performance, provide flexibility and require limited standardization efforts. Additionally, the contribution in [28] demonstrates significant gains due to both vertical sectorization and vertical beamforming in terms of the average and cell-edge throughputs, both in bursty traffic as well as full buffer traffic scenarios.

The main challenge in implementing 3D beamforming is to obtain the accurate 3D channel models which can support the elevation dimension. While extending the current 2D channel model to 3D channel model, the height of the base station and user equipment as well as the downtilt of the antennas should be taken into account. The antenna modelling should include the vertical dimension and the scatterers are supposed to distribute randomly in the 3D space. Therefore, the departure and arrival angles have to be modelled in both horizontal direction and vertical directions [29].

Despite increasing research interest towards 3D BF in the terrestrial paradigm, the application of 3D BF to hybrid satellite-terrestrial coexistence scenarios is quite new. In this context, authors in [30] investigated the application of 3D BF for the spectral coexistence of FSS and FS systems in the Ka shared band (17.7-19.7 GHz). The unique directional properties of SatCom systems can be exploited in order to enable

the spectral coexistence of satellite and terrestrial networks [31][32]. Furthermore, the elevation angle of a satellite terminal can be considered as an additional dof for enabling the spectral coexistence scenarios [30]. In the considered SANSA scenarios, specifically in the urban scenario, 3D BF becomes significantly applicable in order to distinguish the SANSA towers spatially which are located on the same azimuthal plane but at different elevation angles. Similar to different advantages obtained in the access-side, this will allow to minimize intra/inter system interference and subsequently to enhance the backhaul capacity of the SANSA system.

Figure 13 presents a sample result for 3D beam pattern obtained using a Multiple-input Low Noise Block Downconverter (MLNB) based Feed Array Reflector (FAR) configuration [30]. In this evaluation, a Linearly Constrained Minimum Variance (LCMV) beamforming algorithm is employed at the FSS terminal considering the spectral coexistence of FSS-FS systems and a sector-based mitigation approach is followed. In order to apply an LCMV algorithm, it is assumed that the interfering sector is known but exact interfering locations within the considered sector are unknown. As depicted in Figure 13, the interference coming from the considered interfering sector is effectively mitigated using the employed 3D LCMV approach.

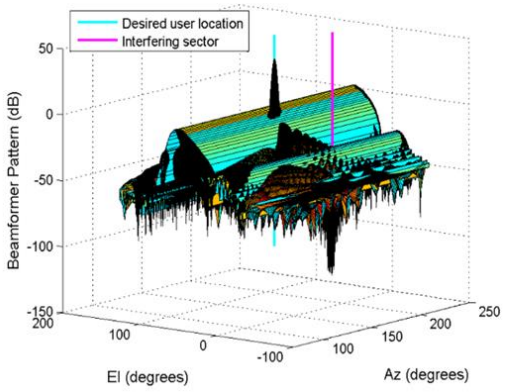

Figure 13: A sample result for 3D pattern with an FAR having 7 LNBs [30]

5.3 Benchmarking topologies

5.3.1 Rural topologies.

In this section, we choose a typical topology from the Finnish 28 GHz database obtained by the University of Luxembourg. It provides a good example to perform some interference and availability analysis. In the next subsection, first we present the chosen topology located in Helsinki. Note that even though Helsinki is a big city, in general it consists of small height buildings. Moreover, the suburban area of Helsinki examined here presents quite sparse building population which is a typical characteristic of a rural environment.

5.3.1.1 Topology Example: Helsinki

The selected topology is depicted in Figure 14. As we can see this topology consists of a number of interconnected star topologies. This topology based on the actual data in the database is composed of 28 links and 15 actual locations (nodes). In Table 3, we may see the underlying parameters defining each link as derived from the Finnish database. Further, Table 3, presents the location of each node. It should be noted that all depicted links are bidirectional.

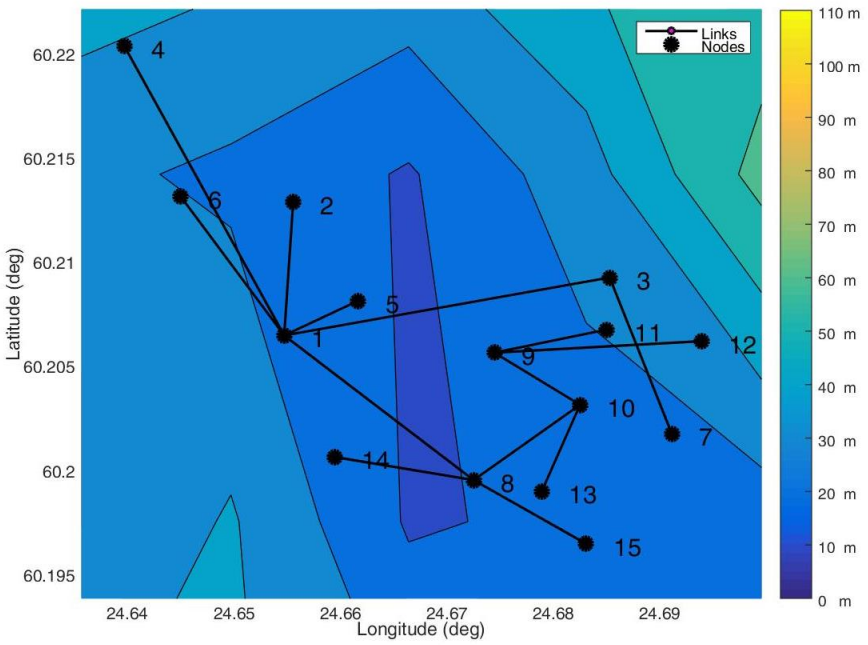

Figure 14: Example backhaul topology obtained from the Finnish 28 GHz database, Helsinki.

5.3.1.2 Benchmark SINR distribution

In this section, we employ the ITU-R 452-16 interference modelling, including the free space loss as well as the diffraction loss based on the Bullington model to derive the SINR of each receiver based on the coordinated frequency plan in Table 4. This result which will be considered as the benchmark SINR distribution is presented in Figure 15. We can see that all the receivers experience SINR > 42dB, while a significant number of them experience SINR > 60dB. This is to be expected since the benchmark topology is the outcome of careful network planning through link registration by the national regulator.

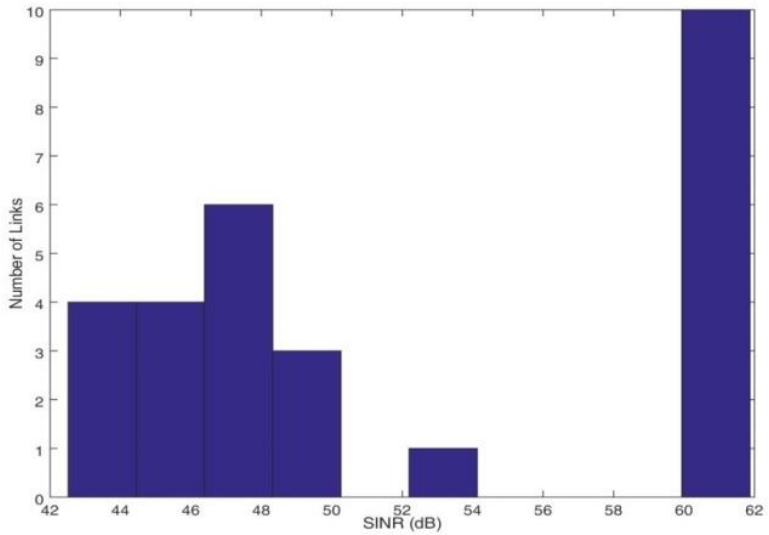

Figure 15: Benchmark SINR distribution of the coordinated frequency plan in Table 4

5.3.1.3 SINR and interference analysis: Aggressive Frequency Reuse

In this section, we will move towards the concept of shared access promoted by SANSA, and analyse the performance of each link, when all employ the same

frequency plan. It should be noted that this is a worst case scenario and less aggressive frequency reuse could be used in practice. We further would like to estimate the number of required nulls to be produced by each SANSA smart antennas to tackle the strong interferers. Here, we define the strong interferers based on the ITU-R recommendations [33]. An interferer is considered to be harmful if the level of received interference increases the noise floor by 10%.

Figure 16 depicts the SINR distribution of the links when full frequency reuse is employed. We can note that in this case the lower value of SINR is reduced to around 22dB from 42dB in the benchmark model. Further, none of the links experience SINR > 48dB. This is explained by the increased internal interference among the SANSA links. It should be noted that further degradation might be experienced if inter-system interference from external links is taken into account.

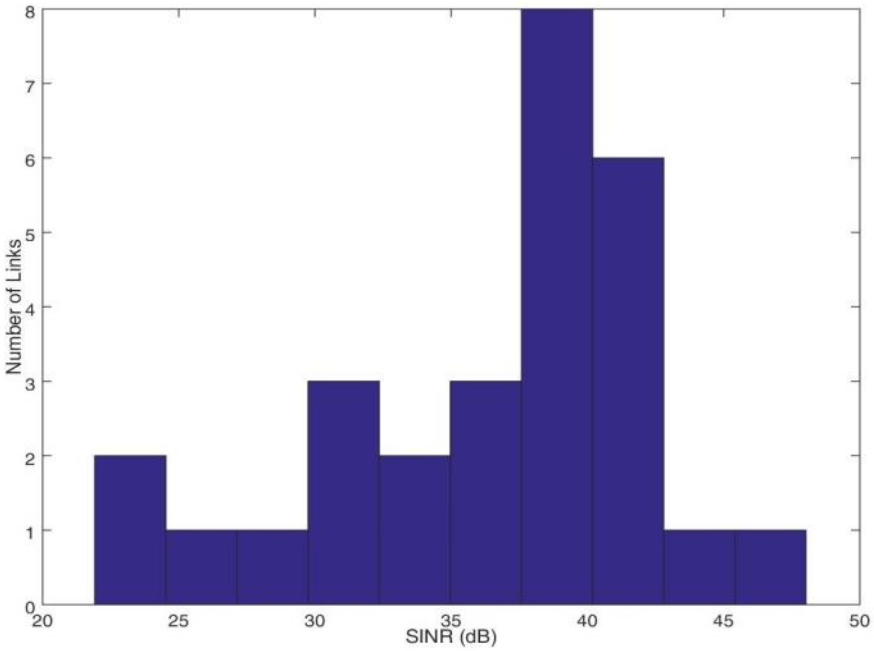

Figure 16: SINR distribution of the links with aggressive frequency reuse

To evaluate the number of strong interferers in each link and thus the required number of nulls in each SANSA designed smart antenna, we can look Figure 17, where the distribution of the number of required nulls is presented. Based on this figure, we can deduce that each node needs to be able to produce 7 nulls in average. It is expected that if less aggressive frequency is used in combination with carrier allocation optimization, a smaller number of nulls will be required. Thus, this number can be considered as an upper bound requirement in SANSA smart antenna techniques.

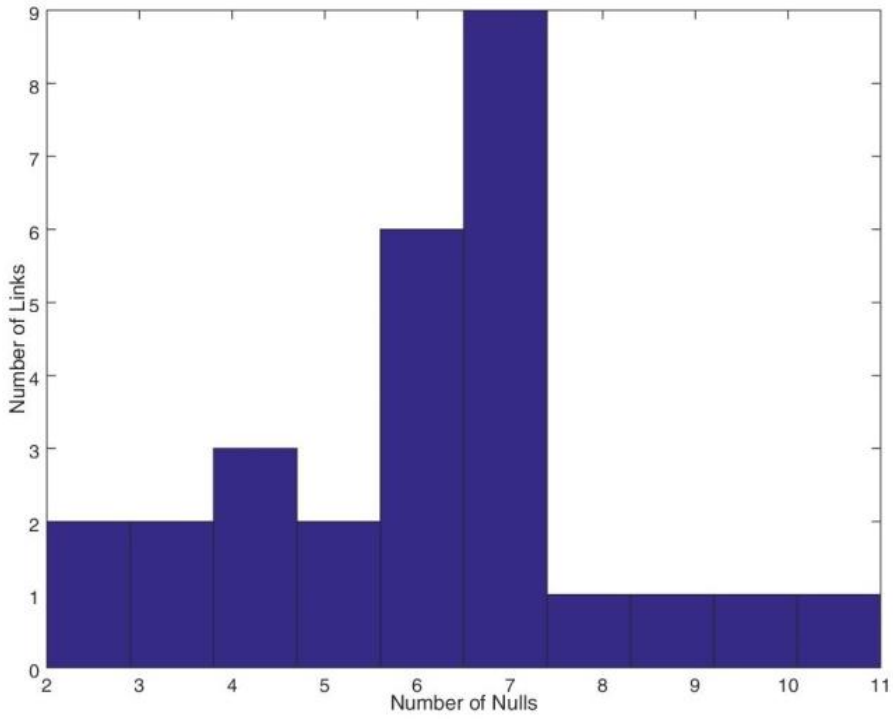

Figure 17: Distribution of the required number of nulls with aggressive frequency reuse

5.3.1.4 Terrestrial to Satellite User Terminal

In this section the impact of employing satellite links for backhauling is studied for the example topology of Section 5.3.1.1. To that end we replace the terrestrial terminals of nodes 1, 8 and 10 of the existing topology with satellite ones and study the interference from the remaining terrestrial nodes. The provided analysis can be considered as a worst case scenario since we assume full frequency reuse and the satellite terminals are placed on the nodes with the largest number of links.

It is assumed that the satellite terminals on these three nodes are pointing to the HYLAS 2 and 31.7^{o} East. Based on the node's position, the satellite antennas should have elevation and azimuth 21.7^{o} and 176^{o} respectively in order to point in this satellite group.

Let us study now the interference generated to the satellite terminals by the terrestrial ones. To that end, in Table 6 we show the aggregated interference that each one of the satellite terminals is experiencing. As we can see, for the specific topology and the elevation angles of the satellite terminals, the interference levels are very low so that there is no need in placing nulls in their direction. The latter is also verified in Table 7 where we show the SINR of each one of the satellite nodes along. Note that for this experimental setup the SNR equals to 10.69dB. As it is shown, each node experiences interference that decreases its SINR less than the 10% of the SNR floor, so based on the ITU-R recommendations the interference can be considered as non- harmful [33]. Note that in cases where the satellite noses are experiencing harmful interference from the terrestrial ones, the latter may apply transmit beamforming techniques in order to null out the interference in the satellite ones.

5.3.1.5 Satellite User Terminal to Terrestrial

Let us now move to the uplink scenario where we are interested for the interference to the terrestrial terminals generated by the satellite ones. It is assumed that the satellite terminals have the same azimuth and elevation parameters to the ones of Section 5.3.1.4. The satellite link characteristics that were used are given in Table 5.

In Figure 18, we plot the distribution of the number of nulls required per terrestrial link due to the transmission of the satellite terminals. The calculations are based again on the ITU-R recommendations [33]. As it is shown, there is requirement for at most one null in only 9 links. The latter result is very promising since the required number of nulls can be easily handled by the antenna infrastructures of the typical backhaul nodes by the application of standard receive beamforming strategies.

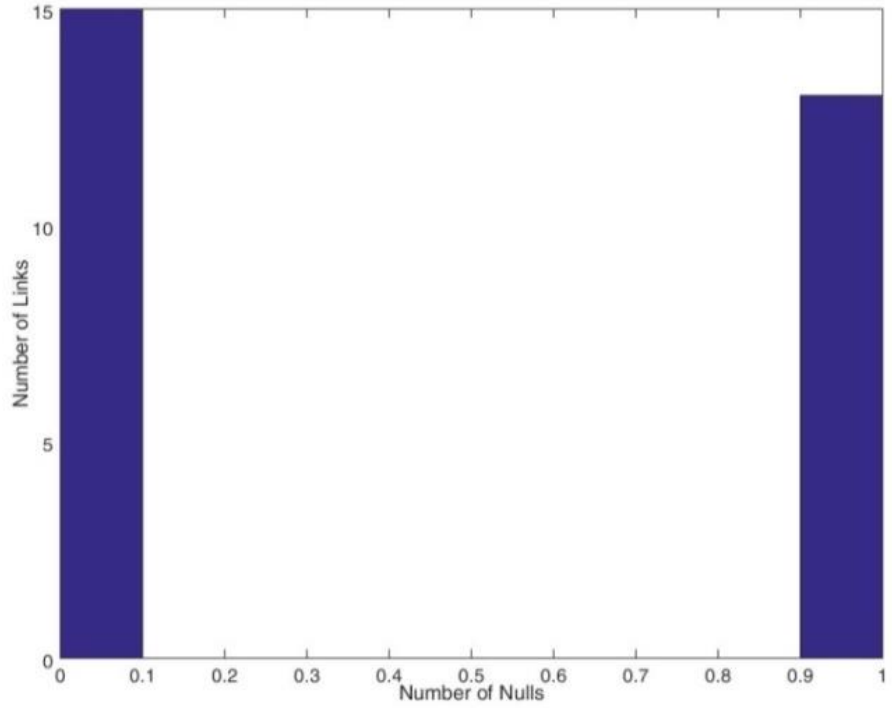

Figure 18: Distribution of the number of nulls per link during uplink

6. Conclusions

This paper shed the light on SANSA approach to enable shared access terrestrial-satellite backhauling. The selected use-cases are presented where different impairments and events have been considered like radio link failure, congestion, new node deployment, remote cell connectivity together with the CDN integration. Additionally, the overall architecture, including the end to end system architecture, the transport architecture as well as the innovative components (HNM and IBN) architecture and the moving base station architecture is provided. The paper covers also the network layer techniques. The interoperability of the terrestrial and the satellite link, the Hybrid Network Manager and the intelligent backhaul nodes as the main network elements in SANSA system, performing the routing and topology configuration functions are explained. Moreover the interference landscape along with a classification of the potential sources of interference and techniques to mitigate its effect and an example of a rural topology are presented. The solutions provided within the frame of this paper are a significant part of the solution proposed

by SANSA in order to help the future backhaul network to satisfy the required traffic demands.

Acknowledgment

This work is supported by the European Commission in the framework of the H2020 SANSA project (Grant agreement no. 645047). The authors acknowledge the contributions of their colleagues in the project.

The project started in February 2015 and has duration of 3 years. As depicted in Figure 19, the involved partners in SANSA are mix of academia (CTTC, ULUX, AIT, Fraunhofer IIS, telecommunications provider (OTE), companies (THALES and VIASAT) and satellite operator (AVANTI).

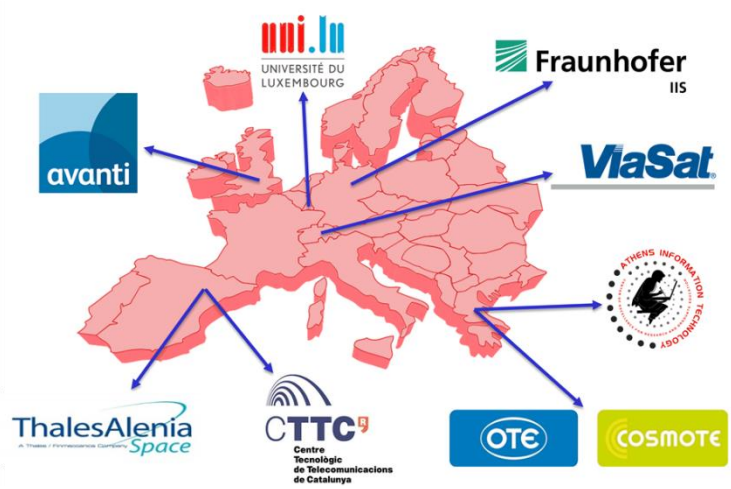

Figure 19: SANSA Partners

References

[1] Digital Agenda for Europe," [Online]. Available: http://ec.europa.eu/digital-agenda/digital-agenda-europe.

[2] ECC/DEC/(00)07 on the shared use of the band 17.7-19.7 GHz by the fixed service and Earth stations of the fixed-satellite service (space-to-Earth)

[3] ECC/DEC/(05)01 on the use of the band 27.5-29.5 GHz by the Fixed Service and uncoordinated Earth stations of the Fixed-Satellite Service (Earth-to-space);

[4] SANSA project, Deliverable 2.1 “Review of Regulatory Environment “, July 2015 , Available at: http://www.sansa-h2020.eu

[5] BATS project, Deliverable 8.3.1, “Regulatory Roadmap“, December 2015, Available at: http://www.batsproject.eu

[6] GPRS enhancements for E-UTRAN access (can be found here http://www.3gpp.org/DynaReport/23401.htm)

[7] 3GPP TS 36.413, S1 Application Protocol (can be found here http://www.3gpp.org/DynaReport/36423.htm)

[8]] 3GPP TS 29.281 General Packet Radio System (GPRS) Tunnelling Protocol User Plane (GTPv1-U) (can be found here http://www.3gpp.org/DynaReport/29281.htm

[9] M. Bengtsson and B. Ottersten,“Optimal and Suboptimal Transmit beamforming,” in Handbook of Antennas in Wireless Communications, L. C. Godara, Ed. CRC Press, 2001.

[10] Q. H. Spencer, A.L. Swindlehurst, and M. Haardt, ``Zero-forcing Methods for Downlink Spatial Multiplexing in Multiuser MIMO Channels," IEEE Transactions on Signal Processing}, vol. 52, no. 2, pp. 461-471, February 2004

[11] M. Bengtsson and B. Ottersten, ``Optimal and Suboptimal Transmit beamforming,” Handbook of Antennas in Wireless Communications, L. C. Godara, Ed. CRC Press, 2001.

[12] C. Masouros and E. Alsusa, “Dynamic Linear Precoding for the exploitation of Known Interference in MIMO Broadcast Systems,” IEEE Transactions On Communications, vol. 8, no. 3, pp. 1396 - 1404, March 2009.

[13] C. Masouros, “Correlation Rotation Linear Precoding for MIMO Broadcast Communications,” IEEE Transactions on Signal Processing, vol. 59, no. 1, pp. 252 - 262, January 2011

[14] M. Alodeh, S. Chatzinotas, and B. Ottersten, "A multicast approach for constructive interference precoding in MISO downlink channel," *IEEE International Symposium on Information Theory (ISIT),* pp.2534-2538, June 29 2014-July 4 2014

[15] M. Alodeh, S. Chatzinotas, and B. Ottersten, "Constructive Multiuser Interference in Symbol Level Precoding for the MISO Downlink Channel," *IEEE Transactions on Signal Processing*, vol.63, no.9, pp.2239-2252, May, 2015.

[16] M. Alodeh, S. Chatzinotas, and B. Ottersten,``Energy Efficient Symbol-Level Precoding in Multiuser MISO Channels,” IEEE International Workshop on Signal Processing Advances in Wireless Communications (SPAWC), Stockholm, Sweden, 2015.

M. Alodeh, S. Chatzinotas, and B. Ottersten, “Energy-Efficient Symbol-Level Precoding in Multiuser MISO Based on Relaxed Detection Region”, IEEE Transactions on Wireless Communications, submitted January 2015.

[17] M. ALODEH, S. CHATZINOTAS, and B. Ottersten, ``Symbol-based precoding in the downlink of MISO cognitive channels,” International Conference on Cognitive Radio Oriented Wireless Networks (CROWNCOM), Doha, Qatar, 2015.

[18] M. Alodeh, S. Chatzinotas, and B. Ottersten, ``Symbol-level precoding for M-QAM modulation in the downlink of MISO channels," IEEE Global Conference on Communications, (GLOBECOM), San Diego, CA, 2015.

[19] M. Alodeh, S. Chatzinotas, and B. Ottersten, "Symbol Level Precoding for Multi-level Adaptive Modulation: A Multicast View", IEEE Journal on Selected Areas on Communications, submitted 2015.

[20] M. ALODEH, S. CHATZINOTAS, and B. Ottersten, `` System and Method for Symbol-level Precoding in Multiuser Broadcast Channels", filed EP15186548.

[21] N. D. Sidropoulos, T. N. Davidson, and Z.-Q. Luo, ``Transmit Beamforming for Physical-Layer Multicasting," IEEE Transactions on Signal Processing, vol. 54, no. 6, pp. 2239-2251, June 2006.

[22] Christopoulos, D.; Chatzinotas, S.; Ottersten, B., "Weighted Fair Multicast Multigroup Beamforming Under Per-antenna Power Constraints," in Signal Processing, IEEE Transactions on , vol.62, no.19, pp.5132-5142, Oct.1, 2014

[23] S. Mohammad Razavizadeh, M. Ahn, and I. Lee, "Three-dimensional beamforming: A new enabling technology for 5g wireless networks," *Signal Processing Magazine, IEEE*, vol. 31, no. 6, pp. 94–101, Nov 2014.

[24] H. Halbauer, S. Saur, J. Koppenborg, and C. Hoek, "3D beamforming: Performance improvement for cellular networks," *Bell Labs Technical Journal*, no. 2, pp. 37–56, Sept 2013.

[25] J. Koppenborg, H. Halbauer, S. Saur, and C. Hoek, "3D beamforming trials with an active antenna array," in *Smart Antennas (WSA), 2012 International ITG Workshop on*, March 2012, pp. 110–114.

[26] J. Xu and J. Zhang, "An attempt to 3D capon beamforming," in *8th International ICST Conference on Communications and Networking in China (CHINACOM)*, Aug 2013, pp. 734–739.

[27] Y. Song, X. Yun, S. Nagata, and L. Chen, "Investigation on elevation beamforming for future LTE-advanced," in *Communications Workshops (ICC), 2013 IEEE International Conference on*, June 2013, pp. 106–110.

[28] F. W. Vook, T. A. Thomas, and E. Visotsky, "Elevation beamforming with beamspace methods for LTE," in *Personal Indoor and Mobile Radio Communications (PIMRC), 2013 IEEE 24th International Symposium on*, Sept 2013, pp. 554–558.

[29] A. Kammoun, H. Khanfir, Z. Altman, M. Debbah, and M. Kamoun, "Preliminary results on 3d channel modeling: From theory to standardization," *Selected Areas in Communications, IEEE Journal on*, vol. 32, no. 6, pp. 1219–1229, June 2014.

[30] S. K. Sharma, S. Chatzinotas, J. Grotz, and B. Ottersten, "3D Beamforming for Spectral Coexistence of Satellite and Terrestrial Networks," in *IEEE VTC-Fall*, Sept. 2015.

[31] S. K. Sharma, S. Chatzinotas, B. Ottersten, "Transmit Beamforming for Spectral Coexistence of Satellite and Terrestrial Networks", in *Proc. Int. Conf. CROWNCOM 2013*, Washington DC, USA, July 2013.

[32] S. K. Sharma, S. Chatzinotas, B. Ottersten, "Spatial Filtering for Underlay Cognitive SatComs", in *Proc. Int. Conf. PSATS 2013*, Toulouse, France, June 2013.

[33] Recommendation ITU-R F.758-6: System parameters and considerations in the development of criteria for sharing or compatibility between digital fixed wireless systems in the fixed service and systems in other services and other sources of interference.

[34] Caini, C., and Firrincieli, R. TCP hybla: a TCP enhancement for heterogeneous networks. International Journal of Satellite Communication and Networking 22, 5 (September 2004), 547–566.

[35] The Ns-3 network simulator, https://www.nsnam.org/
[36] LENA: LTE-EPC Network Simulator, http://networks.cttc.es/mobile-networks/software-tools/lena/
[37] http://www.batsproject.eu
[38] SANSA project, Deliverable 2.2 "State-of-the-art of cellular backhauling technologies ", July 2015 , Available at: http://www.sansa-h2020.eu
[39] http://www.gsma.com/spectrum/wp-content/uploads/2014/12/Wireless-Backhaul-Spectrum-Policy-Recommendations-and-Analysis-Report.-Nov14.pdf
[40] Kreutz, D., et al. "Software-defined networking: A comprehensive survey." Proceedings of the IEEE vol. 103.1, pp. 14-76, 2015
[41] SANSA project, Deliverable 2.3 "Definition of reference scenarios, overall system architectures, research challenges, requirements and KPIs ", January 2016 , Available at: http://www.sansa-h2020.eu

List of tables

Table 1: SANSA selected scenarios

	Spectrum Sharing		Satellite Carrier Bandwidth			Content Delivery Networks			Terrestrial Links	
Scenario ID	**DL only**	**UL+DL**	**SoTA**	**NG HTS**	**UWB**	**No CDN**	**Sat. only multicast**	**Sat.+Terr.Multicast**	**18GHz**	**28GHz**
Rural 1	*		*						*	
Rural 2		*	*	*			*		*	*
Urban 1	*		*				*		*	*
Urban 2	*			*				*	*	*
Urban 3		*			*				*	*
Moving Base Station	*		*			*				*

Table 2: SANSA end-to-end KPIs and targets

KPI	**Target**
Aggregated throughput	Additional satellite capacity
Backhaul network resiliency	SANSA reconfigured network up and ready in <10 seconds.
Delay	Per service type targets Expected improvements of up to 20-30% over SoTA routing solutions especially under backhaul environments.
Spectrum efficiency	10-fold improvement within the considered Ka band segments.
Energy efficiency	Up to 30% improvement compared to benchmark.
Coverage	95-99% EU coverage

Table 3: Detailed information of each link

Link_No	Node_Tx	Node_Rx	Longitude_Tx	Longitude_Rx	Altitude	Azimuth	Elevation	TxFreq	RxFreq	BW	GainMax	Height
1	1	2	24.655	24.656	27.438	3.7	3.0916	29.424	28.416	56	38	48
2	2	1	24.656	24.655	24.847	183.7	-3.098	28.416	29.424	56	38	12
3	1	3	24.655	24.685	27.438	79.6	0.80176	29.369	28.36	56	38	48
4	3	1	24.685	24.655	32.101	259.6	-0.81719	28.36	29.369	56	38	19
5	1	4	24.655	24.64	27.438	331.8	0.28452	29.369	28.36	56	38	48
6	4	1	24.64	24.655	39.472	151.8	-0.30028	28.36	29.369	56	38	27
7	1	5	24.655	24.662	27.438	64.2	5.3209	29.313	28.305	56	38	48
8	5	1	24.662	24.655	21.549	244.2	-5.3247	28.305	29.313	56	38	14
9	1	6	24.655	24.645	27.438	324.1	2.066	29.313	28.305	56	38	48
10	6	1	24.645	24.655	30.249	144.1	-2.0743	28.305	29.313	56	38	12
11	7	3	24.691	24.685	26.502	338.9	-0.93673	29.369	28.36	56	38	10
12	3	7	24.685	24.691	32.101	158.9	0.92868	28.36	29.369	56	38	19
13	8	1	24.672	24.655	20.097	308.2	-1.712	28.249	29.256	56	38	18
14	1	8	24.655	24.672	27.438	128.2	1.7007	29.256	28.249	56	38	48
15	9	10	24.674	24.682	20.448	122	-1.164	28.416	29.424	56	38	18
16	10	9	24.682	24.674	26.113	302	1.1593	29.424	28.416	56	38	23
17	9	11	24.674	24.685	20.448	78	-0.91477	28.36	29.369	56	38	18
18	11	9	24.685	24.674	29.969	258	0.90941	29.369	28.36	56	38	18
19	9	12	24.674	24.694	20.448	86.7	-0.45421	28.305	29.313	56	38	18
20	12	9	24.694	24.674	34.914	266.7	0.44454	29.313	28.305	56	38	12
21	13	10	24.679	24.682	21.247	23.3	-1.7998	28.305	29.313	56	38	12
22	10	13	24.682	24.679	26.113	203.3	1.7953	29.313	28.305	56	38	23
23	8	10	24.672	24.682	20.097	54	-0.92413	28.416	29.424	56	38	18
24	10	8	24.682	24.672	26.113	234	0.91799	29.424	28.416	56	38	23
25	8	14	24.672	24.659	20.097	279.7	-0.44412	28.416	29.424	56	38	18
26	14	8	24.659	24.672	25.748	99.7	0.43754	29.424	28.416	56	38	18
27	8	15	24.672	24.683	20.097	120.2	0.30092	28.416	29.424	56	38	18
28	15	8	24.683	24.672	22.504	300.2	-0.30699	29.424	28.416	56	38	12

Table 4: The location of nodes

Node_No	Latitude	Longitude
1	60.206	24.655
2	60.213	24.656
3	60.209	24.685
4	60.22	24.64
5	60.208	24.662
6	60.213	24.645
7	60.202	24.691
8	60.199	24.672
9	60.206	24.674
10	60.203	24.682
11	60.207	24.685
12	60.206	24.694
13	60.199	24.679
14	60.201	24.659
15	60.196	24.683

Table 5: Simulation parameters for uplink

Parameter	Value
B^{FSS}	7 MHz
Shared band	$27.5 - 29.5$ GHz (285 carriers)
Exclusive band	$29.5 - 30$ GHz (71 carriers)
Parameters for FSS system	
Satellite location	13°E
EIRP FSS terminal	50 dBW
$G_{\text{Rx}}^{\text{SAT}}(k)$	Between 44.43 and 57.88 dBi
$[C/I_{\text{rtn}}^{\text{co}}]$	Between 5.80 and 20.74 dB
Reuse pattern	4 color (freq./pol.)
Satellite height	35,786 Km
$G_{\text{Tx}}^{\text{FSS}}(0)$	42.1 dBi
N_0	-131.78 dBW
Terminal height	15 m

Table 6: Aggregate Interference on the satellite terminals due to terrestrial transmissions

Node Number	1	8	10
Aggregate Interference (dB)	-140.84	-140.78	-143.21

Table 7: SINR of the satellite terminals

Node Number	1	8	10
SINR	10.55	10.54	10.60

Biographies

Georgios Ziaragkas

Georgios is working as a Satellite Communications Engineer for Avanti Communications. His main scientific interests are hybrid satellite terrestrial technologies and Internet of Things. He is also working on sustainable business modelling for innovative technological projects. Georgios is currently involved in European FP7 and H2020 projects. He has also worked as a satellite ground station engineer focused on satellite earth communications and computer networks. He holds a MEng. in Electrical & Computer Engineering from Aristotle University of Thessaloniki, with his main scientific focus being on Ultra-Wideband (UWB) communications and a Master in Business Administration (M.B.A.) from Athens University of Economics and Business.

Georgia Poziopoulou

Georgia is currently working as a Satellite Communications Engineer in Avanti Applied Technologies group. She joined Avanti in 2013 as a Graduate Engineer and has since worked in ApTec making technical contributions to existing projects and supporting new bids. She has also completed a placement in the Satellite Resource Management team performing link budget analyses and supporting everyday operations. She holds a MSc. in Wireless and Optical Communications from University College London from which she graduated in 2013 with Distinction and a MEng. in Electrical and Computer Engineering from the National Technical University of Athens in Greece. The research projects she has completed during her university studies were focused on power efficiency of linear precoding in MIMO systems and energy efficient communication in Wireless Sensor Networks with the use of time-scheduling and clustering algorithms.

José Núñez-Martínez

José Núñez-Martínez is currently a Senior Researcher in the Mobile Networks Department at CTTC in Barcelona (http://networks.cttc.es/mobile-networks/). He received a MSc (2005) degree in Computer Science Engineering from the Technical University of Catalonia (UPC) and the PhD (2014) from the Computer Architecture Department of the same university (http://www.upc.edu). From 2004 until September 2007, he worked as Network Engineer in the Advanced Broadband Communication Center (CCABA) of UPC. He joined CTTC in September 2007 as software network engineer. He has participated in several national (Cicyt), European (FP7), and industrial projects (Ditech, and AVIAT). He is author and co-author of more than 30 research papers. His current research interests include: wireless backhaul, small cells, network protocols, self-organization, network optimization, and network function virtualization.

Jorge Baranda Hortigüela

Jorge Baranda Hortigüela is currently a Researcher in the Mobile Networks Department at CTTC in Barcelona. He received an Msc (2008) degree in Electrical Engineering from the Technical University of Catalonia. Before joining CTTC in November 2009, he did an internship at Philips Research (Eindhoven, The Netherlands). At CTTC, he has participated in several national (Cicyt), European (FP7, H2020), and industrial projects (AT4). His main research interests are focused on different aspects of networking: Software Defined Networking (SDN), Network Function Virtualization (NFV) and how these trends can complement former distributed networking concepts like efficient routing in wireless backhaul networks.

Isaac Moreno

Isaac Moreno obtained his Bachelor of Science in Physics in the UCM of Madrid in 1996. He works currently as Systems Engineer in the SW & Ground product line in Thales Alenia Space España. His areas of work are related to the development and definition of the Network Management System, as part of the Ground Segment systems. He is expert in specification, development and validation of satellite communication systems, having participated in multiple programs related to satellite interactive systems, as REDSAT, AmerHis (ESA Project), IBIS, SatLife, Healthware or Geocast (IST Projects). Isaac has been involved in the TM-RCS DVB working group and participated actively in the specification of the DVB-RCS2 standards. Previously, he worked in Alcatel as validation and SW design engineer in projects related to ADSL product, VoIP and fixed Switching Exchanges.

Christos Tsinos

Christos Tsinos received the Diploma degree in computer engineering and informatics, the MSc and the PhD degree in signal processing and communication systems and MSc in applied mathematics from the University of Patras, Greece, in 2006, 2008, 2013 and 2014 respectively. From August 2014 to June to 2015 he was a Postdoctoral Researcher at University of Patras. Since July 2015 he joined as a Research Associate the Interdisciplinary Centre for Security, Reliability and Trust (SnT), University of Luxembourg, Luxembourg. He is currently involved or was involved in the past in a number of different R&D projects funded by national and/or EU funds. His current research interests include mmWave communications, cognitive radio, adaptive and distributed signal processing. Dr. Tsinos is a member of the Technical Chamber of Greece.

Sina Maleki

Sina Maleki received his PhD degree from Delft University of Technology, Delft, The Netherlands, in 2013, and his MSc from the same university in 2009. From July 2008 to April 2009, he was an intern student at the Philips Research Center, Eindhoven, The Netherlands, working on spectrum sensing for cognitive radio networks. Since August 2013, he has been working at the Interdisciplinary Centre for

Security, Reliability and Trust, University of Luxembourg, where he is working on cognitive radio for satellite communications as well as interference monitoring and localization in satellite systems within the EU H2020 and FP7 projects SANSA and CoRaSat, as well as Luxembourgish national projects CO2SAT, SeMIGod, and SATSENT. He is further involved in European Space Agency projects SATNEX IV and ASPIM.

Shree Krishna Sharma

Shree Krishna Sharma received the M.Sc. degree in information and communication engineering from the Institute of Engineering (IoE), Pulchowk, Nepal; the M.A. degree in economics from Tribhuvan University, Nepal; the M.Res. degree in computing science from Staffordshire University, Staffordshire, U.K.; and the Ph.D. degree in Wireless Communications from University of Luxembourg, Luxembourg. Since November 2014, he has been working as a Research Associate in Interdisciplinary Centre for Security, Reliability and Trust (SnT), University of Luxembourg, Luxembourg. He is the author of more than 50 technical papers in refereed international journals, scientific books, and conferences. He received an Indian Embassy Scholarship for his B.E. study, an Erasmus Mundus Scholarship for his M. Res. study, and an AFR Ph.D. grant from the National Research Fund of Luxembourg. He received Best Paper Award in International Conference on Cognitive Radio Oriented Wireless Networks (CROWNCOM) 2015 held in Doha, Qatar. For his Ph.D. thesis, he received FNR award for outstanding PhD Thesis 2015 from National Research Fund (FNR), Luxembourg. His research interests include cognitive wireless communications, satellite communications, and signal processing techniques for 5G and beyond wireless.

Maha Alodeh

Maha Alodeh (S'11, M'16) received her bachelor degree in electrical engineering from University of Jordan, Amman, Jordan in 2010, and her Ph.D. degree in electrical engineering from the Interdisciplinary center for Security and Trust, (SnT), University of Luxembourg in 2016. Alodeh's research interests includes signal processing for wireless and satellite communications with focus on interference management and cognitive radio.

Symeon Chatzinotas

Symeon Chatzinotas (S'06-M'09-SM'13) received the M.Eng. in Telecommunications from Aristotle University of Thessaloniki, Greece and the M.Sc. and Ph.D. in Electronic Engineering from University of Surrey, UK in 2003, 2006 and 2009 respectively. He is currently a Research Scientist with the research group SIGCOM in the Interdisciplinary Centre for Security, Reliability and Trust, University of Luxembourg, managing H2020, ESA and FNR projects. In the past, he has worked in numerous R&D projects for the Institute of Informatics & Telecommunications, National Center for Scientific Research Demokritos, the Institute of Telematics and Informatics, Center of Research and Technology Hellas and Mobile Communications Research Group, Center of Communication Systems Research, University of Surrey.

He has authored more than 180 technical papers in refereed international journals, conferences and scientific books. His research interests are on multiuser information theory, cooperative/cognitive communications and wireless networks optimization. Dr Chatzinotas is the co-recipient of the 2014 Distinguished Contributions to Satellite Communications Award, Satellite and Space Communications Technical Committee, IEEE Communications Society and the 2016 CROWNCOM Best Paper Award. He has coedited a book on ”Cooperative and Cognitive Satellite Systems” has co-organized the First International Workshop on Cognitive Radios and Networks for Spectrum Coexistence of Satellite and Terrestrial Systems (CogRaN-Sat) in conjunction with the IEEE ICC 2015, 8-12 June 2015, London, UK.